DOI 10.1007/s11595-015-1200-z

# Wear and Corrosion Resistance of Electroless Plating Ni-P Coating on P110 Steel

**LIN Naiming[1], ZHOU Peng[1], ZOU Jiaojuan[1], XIE Faqin[2], TANG Bin[1]**

*(1. Research Institute of Surface Engineering, Taiyuan University of Technology, Taiyuan 030024, China; 2.School of Aeronautics, Northwestern Polytechnical University, Xi'an 710072, China)*

**Abstract:** In order to improve the surface performance and increase the lifetime of P110 oil casing tube steel during operation, electroless plating was conducted to form Ni-P coating onto its surface. The surface morphology/element distribution and phase constitution of the Ni-P coating were analyzed using scanning electron microscope (SEM) equipped with energy dispersive spectrometry (EDS) and X-ray diffraction (XRD). Tribological and electrochemical measurement tests were applied to investigate the wear and corrosion resistance of P110 steel and the Ni-P coating. The results showed that a uniform and compact, high phosphorous Ni-P coating was formed. The obtained Ni-P coating indicated certain friction-reduction effect and lower mass loss during friction-wear tests. The Ni-P coating also exhibited higher corrosion resistance in comparison with bared P110 steel. The obtained Ni-P coating has significantly improved the surface performance of P110 steel.

**Key words:** wear; corrosion; electroless plating; Ni-P coating; P110 steel

## 1 Introduction

The petroleum tube is an important structural unit of an oil/gas well, it usually spends one-third of the entire oil well development cost while the oil casing tube takes 73%-76% of the total petroleum tube consumption[1,2]. Oil casing tubes are prone to deteriorate under the complex and adverse work conditions in oil/gas wells[1,2]. It has been reported that oil casing tubes directly influence the service time of oil well, and the oil well would determine the oil field lifetime[1]. Based on the understanding about the corrosion of oil casing tube, several corrosion protection approaches: utilization of anticorrosion alloy, injecting inhibitor, cathode protection and surface treatments have been proposed[3]. Surface treatments have the advantage of providing a compromise between the performance and the cost to resist corrosion and/or wear with further properties to prevent or reduce the wastage of materials[4]. Our group concentrated on improving the surface properties of plain carbon steel oil casing tube by surface treatment that can satisfy the requirements of operations for petroleum production. Due to the excellent properties of Ni-P alloy coating such as good corrosion resistance, promising wear-resistance and high hardness, electroless plating Ni-P coating has been extensively applied in many fields. Another advantage of the electroless plating technique is that much uniform coating can be obtained without special requirements for substrate geometries[5,6].

In this paper, a Ni-P alloy coating has been deposited on P110 oil casing tube steel (P110 steel) in order to improve the surface performance and increase the lifetime during operation. The wear and corrosion resistance of P110 steel and the Ni-P coating have been estimated.

## 2 Experimental

The specimens used for the experiments were cut into 25 mm×20 mm×3 mm plates by an electro-spark wire-electrode cutting machine from the P110 steel oil casing tube. The chemical composition (wt%) of the P110 steel was: C 0.26; Si 0.19; Mn 1.37; P 0.009; S 0.004; Cr 0.148; Ni 0.028; Mo 0.013; Cu 0.019; Nb 0.06; V 0.006; Ti 0.011; and Fe balance. The raw samples were finely ground using SiC abrasive paper, followed by ultrasonic cleaning in an acetone bath.



(Received: Jul.05, 2013; Accepted: Feb. 01, 2015)

LIN Naiming(林乃明): Ph D; E-mail: lnmlz33@126.com

Funded by the China Postdoctoral Science Foundation (No.2012M520604), the Natural Science Foundation for Young Scientists of Shanxi Province (No.2013021013-2)

All the samples were subjected to the following pre-treatment and electroless plating procedure:

Cleaning in alkaline solution containing 70 g/L sodium hydroxide, 40 g/L sodium carbonate, 20 g/L sodium phosphate, and 10 g/L sodium silicate, at the temperature of 85 ℃ for 5 min; Immersion in distilled water at room temperature (RT) for 2 min; Cleaning in 20 vol% HCl at RT for 1 min; Rinsing by immersion in distilled water at RT for 2 min; Cleaning in 5 vol% $H_2SO_4$ at RT for 1 min; Rinsing by distilled water at RT for 2 min; Electroless plating, dipping into the plating bath whose composition and correlative parameters are given in Table 1; Rinsing by distilled water at RT for 2 min, and drying in the air.

**Table 1 Bath composition for the electroless plating Ni-P coating**

| Chemical compounds | Concentration /(g/L) |
|---|---|
| $NiSO_4 \cdot 6H_2O$ | 30 |
| $NaH_2PO_2$ | 30 |
| $Na_3C_6H_5O_7 \cdot 2H_2O$ | 40 |

* The pH was 9 and the temperature was 85-88 ℃

Scanning electron microscope (SEM) equipped with energy dispersive spectrometry (EDS) was used to assess the surface morphology and surface element distributions of the Ni-P coating. The phase constitution of the coating was identified by X-ray diffraction (XRD) using Co K$\alpha$ radiation ($\lambda$=0.178 9 nm).

The tribological behaviors of P110 steel and Ni-P coating were analyzed on the HT-1000 friction-wear testing machine by a ball-on-disc type tribometer in dry sliding. High carbon chromium bearing steel balls with the diameter of 5 mm were chosen as the counterparts. All the tests were conducted by disc wearing against counter balls at 303 K with a gyration radius of 6 mm, a normal load of 5 N and a sliding velocity of 224 r/min for 30 min. Tribological characteristics of the samples were defined by comparing the results of friction coefficient, mass loss and the wear trace. An analytical balance with an accuracy of 0.01 mg was employed to weigh the original and worn samples. The topographical features of the worn surfaces belonging to the samples were examined using an optical microscope (OM).

The electrochemical techniques of potentiodynamic polarization were monitored in $CO_2$-saturated simulated oilfield brine to make a comparative research on the corrosion resistance of P110 steel and the obtained coating. The chemical composition of the corrosion medium is shown in Table 2[7]. The experiments were performed with the electrochemical measurement system (PARSTAT-2273). The corrosion cell was combined with a typical three-electrode configuration. The saturated calomel electrode (SCE) was used as reference electrode and the counter electrode was a platinum plate. Bare P110 steel and

**Table 2 Concentration of electrolyte in simulated oilfield stratum water**

| Content | $Cl^-$ | $SO_4^{2-}$ | $HCO_3^-$ | $CO_3^{2-}$ | $Na^+$ | $Mg^{2+}$ | $Ca^{2+}$ |
|---|---|---|---|---|---|---|---|
| mg/L | 19 | 1.14 | 0.6 | 0.12 | 11.99 | 1.05 | 0.39 |

coated P110 steel samples were employed as working electrodes with a naked geometric area of 1 $cm^2$. All the tests were conducted inside a thermostat at 303 K. The polarization tests of the samples were performed after they had been soaked in the solution for 1 800 s. The potential of the sample was swept at a rate of 0.5 mV/s. The corrosion current density of each sample was calculated by Tafel extrapolation method from the polarization curves[8].

# 3 Results and discussion

The Ni-P coating exhibits a silver-grey surface by naked-eye glance. Fig.1 presents the surface morphology of Ni-P coating. It is seen that the obtained coating is uniform and compact. It indicates a typical cauliflower-like characteristic of Ni-P coating formed by electroless plating[5, 6].

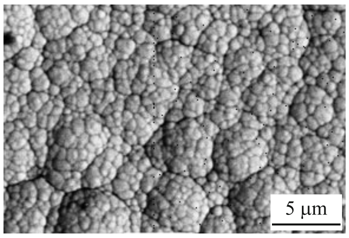


Fig.1 Surface morphology of the Ni-P coating

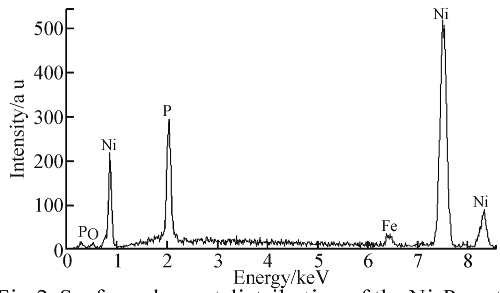


Fig.2 Surface element distribution of the Ni-P coating

The surface element distribution of the Ni-P coating is given in Fig.2 and Table 3, which exhibits the contents of Ni and P, meanwhile minor Fe and O are also detected. According to the content of P in the coating, the obtained Ni-P coating can be classified as a high phosphorous coating.

The XRD pattern of the obtained coating is given in Fig.3. Only a single diffraction peak can be found from the pattern. X-ray diffraction is formed through the crystal faces fitting the Bragg diffraction angle. By comparison with the XRD diffraction profile cards, it can be seen that the coating was composed of amorphous and microcrystalline nickel.

Table 3 Surface element distribution of the Ni-P coating/wt%

| Ni | P | Fe | O |
|---|---|---|---|
| 84.08 | 12.13 | 1.95 | 1.84 |

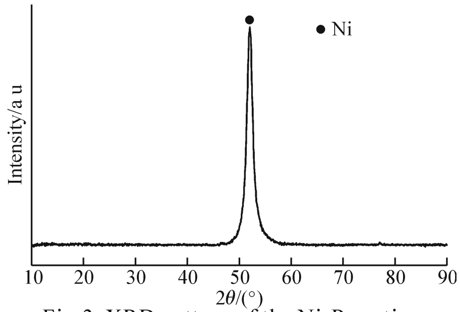

Fig.3 XRD pattern of the Ni-P coating

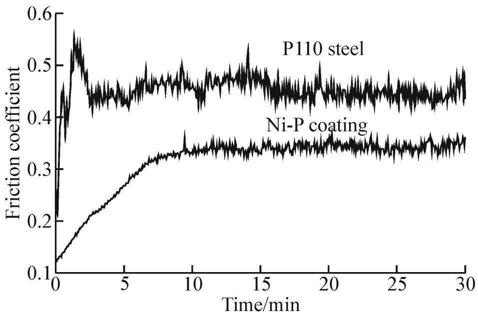

Fig.4 Friction coefficients of the Ni-P coating and P110 steel

Fig.4 illuminates the friction coefficient-time curves of the P110 steel and the Ni-P coating. As shown in Fig.4, the friction coefficient belonging to the P110 steel substrate exhibits a sharp fluctuation characteristic, which indicates the existence of a running-in period during the initial state in sliding. And afterwards the friction coefficient of the P110 steel substrate maintained at a relatively constant level around 0.45. It is noted that in the initial sliding stage the friction coefficient of Ni-P coating continually increased for about 10 min and then reached 0.35. It is seen that the Ni-P coating exhibits a notable friction reduction effect[9]. Meanwhile it can be found that the friction coefficient of Ni-P coating has been consistently lower than the P110 steel substrate, and this reveals that the coating had not been worn out after the sliding test.

Fig.5 and Fig.6 compare the variation characteristics of the surface hardness and mass losses between the P110 steel and Ni-P coating. It is notable that the Ni-P coating has higher surface hardness than that of P110 steel; considerable enhancement in hardness of P110 steel on the surface is connected with the formation of the Ni-P coating. While under the same conditions, the mass loss of the Ni-P coating is far lower than that of P110 steel, as shown in Fig.6. The reduction of mass loss of the coated-P110 steel in dry sliding can be attributed to the higher surface hardness degree and the friction reduction effect of Ni-P coating.

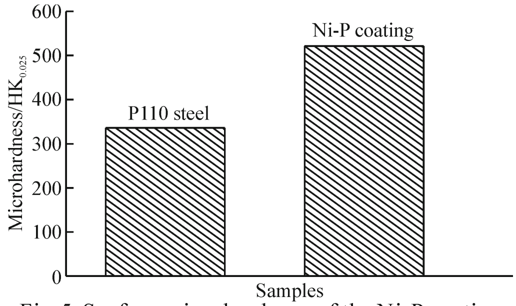

Fig.5 Surface microhardness of the Ni-P coating and P110 steel

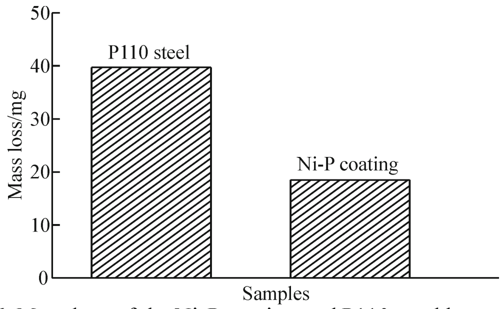

Fig.6 Mass loss of the Ni-P coating and P110 steel by wearing

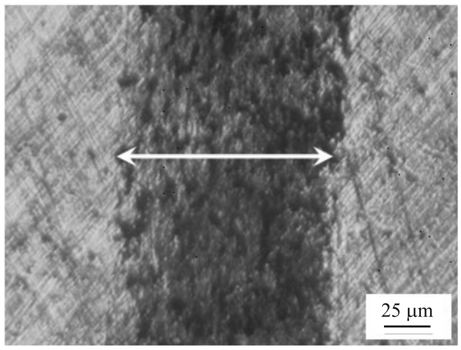

Fig.7 Wear trace of the P110 steel

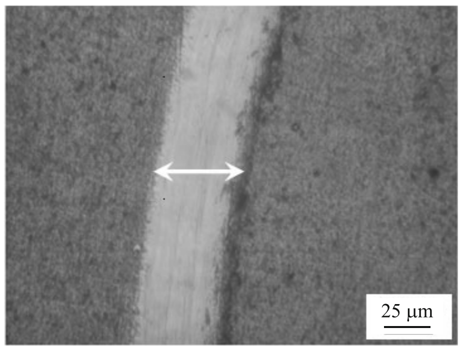

Fig.8 Wear trace of the Ni-P coating

Fig.7 and Fig.8 illustrate the wear scars of P110 steel and the Ni-P coating. Seen from Fig.7, the P110 steel is severely worn. Grooves and indentation can be observed in the wear track, the wear mechanism of P110 steel is abrasive wear. As presented in Fig.8, the wear scar of the Ni-P coating is narrower than that of P110 steel, and the damage in wearing to the Ni-P coating is not as severe as P110 steel, shallow plows are notable, and the wear mode of Ni-P coating is slight abrasive wear[9].

Fig.9 presents the polarization curves of P110 steel and the obtained coating. Table 4 gives the results of the electrochemical tests. From Fig.9 it can be found that the corrosion potential ($E_{corr}$) of the Ni-P coating is much higher than that of the P110 steel, meanwhile the corrosion current density ($I_{corr}$) corresponding to the Ni-P coating is lower in comparison to the P110 steel. It is seen in Fig.9 that P110 steel shows no passive zone, its anodic current increases with increasing polarization. After the polarization test of P110 steel, the corrosion medium became yellowish green, implying that iron cations entered into the solution[10]. The Ni-P coating presents a passivation-like region in the potential domain from -200 to 200 mV with lower corrosion current density than that of P110 steel. Thereafter the corrosion current density kept on increasing. By using the Tafel extrapolation method, a high corrosion current density of 3.322 8E-5 A/cm$^2$ is obtained by P110 steel, and the Ni-P coating reveals a corrosion current density of 5.396E-6 A/cm$^2$. Combining the corrosion potential and corrosion current density in polarization measurements, the Ni-P coating exhibits certain protective effect on P110 steel substrate in the selected corrosion medium.

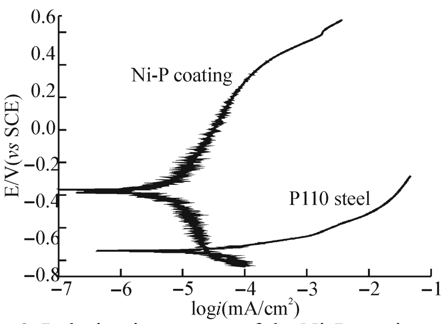

Fig.9 Polarization curves of the Ni-P coating and the P110 steel

**Table 4 Results of the electrochemical tests**

| Samples | $E_{corr}$/V | $i_{corr}$(A/cm$^2$) |
|---|---|---|
| P110 steel | −0.739 | 3.322 8E-05 |
| Ni-P coating | −0.364 | 5.396 6E-06 |

The promising corrosion resistance of the Ni-P coating can be explained from the aspects as follows: (a) the Ni-P coating has a high chemical stability in the corrosion medium and meanwhile plays a mechanical isolation effect; (b) the Ni-P coating is composed of a mixture of amorphous and microcrystalline nickel, there are not so many grain boundaries in the electroless plating Ni-P coating as in crystalline nickel, thus indicating a low corrosion sensitivity; (c) the Ni-P coating exhibits a certain passivating effect in the electrolyte, as illustrated in Fig.10. The formed passivation layer can protect the coating against corrosion. The above results have indicated that the Ni-P coating had a better anticorrosion property than P110 steel in $CO_2$-saturated simulated oilfield brine. Meanwhile P110 steel has benefited from the chemical stability and mechanical isolation effect of Ni-P coating in the corrosion solution[11].

# 4 Conclusions

A continuous high phosphorous Ni-P coating has been formed on P110 steel by electroless plating, which is composed of amorphous and microcrystalline nickel. The Ni-P coating has significantly enhanced the surface hardness of P110 steel. Tribological tests results have confirmed that P110 steel obtains excellent friction reduction property and wear resistance by depositing a Ni-P coating. The wear mechanism of P110 steel is abrasive wear, and the Ni-P coating undergoes slight abrasive wear. The Ni-P coating indicates higher corrosion potential and lower current density, and exhibits better corrosion resistance than P110 steel in $CO_2$-saturated simulated oilfield brine. The protective effect of the Ni-P coating is attributed to its desirable chemical stability and mechanical isolation effect.

**References**

[1] Li H L, Zhang Y P, Han L H. Development Situation of OCTG and Production Localization of Hi-grade OCTG: Part I[J]. *Steel Pipe*, 2007, 36(6): 1-6 (in Chinese)

[2] Li H L, Zhang Y P, Han L H. Development Situation of OCTG and Production Localization of Hi-grade OCTG: Part II [J]. *Steel Pipe*, 2008, 37(1): 1-6 (in Chinese)

[3] Xiong Y, Chen D J. Research on $CO_2$ Corrosion Protection Technology in Oil and Gas Field[J]. *Total Corrosion Control*, 2007, 21(4): 2-4 (in Chinese)

[4] Lin N M, Xie F Q, Wu X Q, *et al*. Review on the Development and Prospect of Surface Protection Technology for Oil Casing Tubes[J]. *Corros. Prot.*, 2009, 30: 801-805 (in Chinese)

[5] Balaraju J N, Sankara Narayanan T S N, Seshadri S K. Electroless Ni-P Composite Coatings[J]. *J. Appl. Eletrochem*., 2003, 33: 807-816

[6] Gu C D, Lian J S, Li G Y, *et al*. Electroless Ni–P Plating on AZ91D Magnesium Alloy from a Sulfate Solution[J]. *J. Alloy Compd*., 2005, 391: 104-109

[7] Chen C F. *Research on Electrochemical Behavior and Corrosion Scale Characteristics of $CO_2$ Corrosion for Tubing and Casing Steel*[D]. Xi'an: Northwestern Polytechnical University, 2002

[8] Liu N, Wang J L, Wang L D, *et al*. Electrochemical Corrosion Behavior of Mg-5Al-0.4Mn-*x*Nd in NaCl Solution[J]. *Corros. Sci.*, 2009, 51: 1 328-1 333

[9] Keshri A K, Agarwal A. Wear Behavior of Plasma-sprayed Carbon Nanotube Reinforced Aluminum Oxide Coating in Marine and High-temperature Environments[J]. *J. Therm. Spray*, 2011, 20: 1 217-1 230

[10] Ye W, Li Y, Wang F H. The Improvement of the Corrosion Resistance of 309 Stainless Steel in the Transpassive Region by Nano-crystallization[J]. *Electrochim. Acta*, 2009, 54: 1 339-1 349

[11] Marin E, Lanzutti A, Guzman L, *et al*. Corrosion Protection of AISI 316 Stainless Steel by ALD Alumina/Titania Nanometric Coatings[J]. *J. Coat. Technol. Res*., 2011, 8: 655-659